

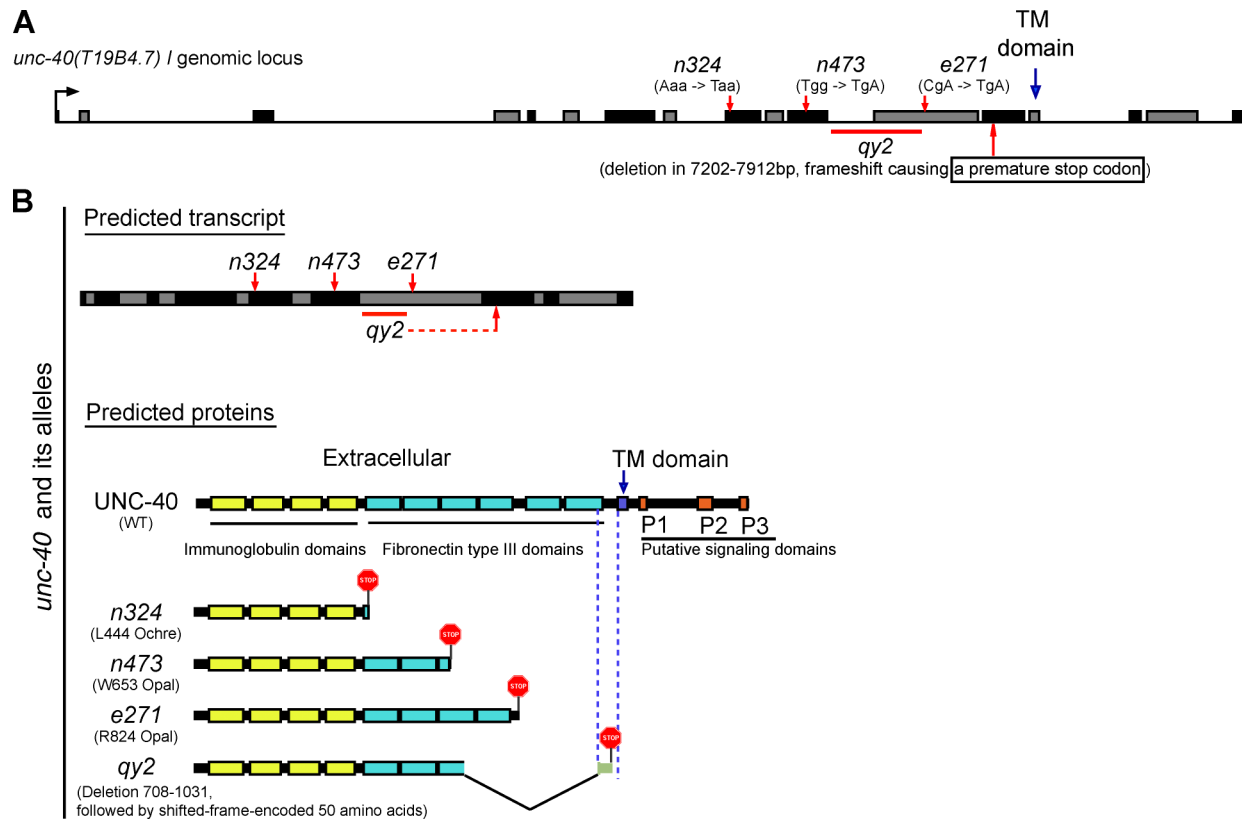
Wang et al., <http://www.jcb.org/cgi/content/full/jcb.201405026/DC1>

Figure S1. **Generation and characterization of *unc-40* alleles.** (A and B) Schematic diagram of *unc-40* mutant alleles. (A) The genomic locus of *unc-40* shows the exons (alternating black and dark gray boxes) and introns (lines between boxes). The locations of putative *unc-40*-null alleles are indicated with red arrows for nonsense mutations and a red line for the deletion. The blue arrow indicates the location of the TM domain. (B) The diagram shows the corresponding locations (red arrows) of these *unc-40* alleles in the predicted transcript of the *unc-40* gene, and the predicted UNC-40 proteins encoded by the wild type and each of the *unc-40* mutant alleles.

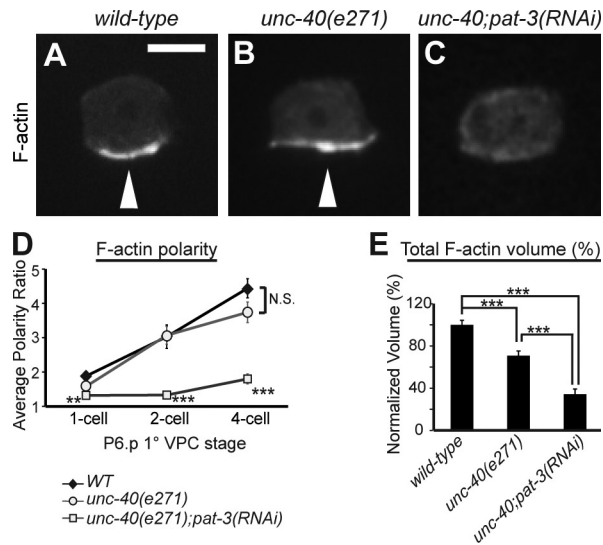


Figure S2. **INA-1/PAT-3 (integrin) mediates *unc-40*-independent polarizing and F-actin-promoting activity at the invasive cell membrane.** Anterior is left; ventral is down. (A–C) All animals were examined at the P6.p four-cell stage. (A) In wild-type animals, F-actin polarizes to the invasive cell membrane (arrowhead). Bar, 5  $\mu$ m. (B) In *unc-40* mutants, there was a reduction, but not loss, of F-actin at the invasive cell membrane of the AC in all cases (arrowhead). (C) RNAi targeting *pat-3*, the  $\beta$  subunit of integrin heterodimer  $\alpha$ INA-1/  $\beta$ PAT-3, reduced F-actin volume and polarization at the invasive membrane in *unc-40* mutants. (D) Quantification of F-actin polarity in the ACs of wild-type (closed diamonds), *unc-40* (open circles), and *unc-40;pat-3(RNAi)* (open squares) animals at the P6.p one-, two-, and four-cell stages ( $n \geq 15$  for each stage per genotype). Significant differences relative to wild-type animals are indicated. (E) Quantification of the total F-actin volume in the ACs in wild type (as a control for normalization), *unc-40*, and *unc-40;pat-3(RNAi)* at the P6.p four-cell stage ( $n \geq 15$  per genotype). \*,  $P < 0.05$ ; \*\*,  $P < 0.01$ ; \*\*\*,  $P < 0.001$ . N.S., no significant difference ( $P > 0.05$ , Student's  $t$  test). Error bars represent  $\pm$  SEM.

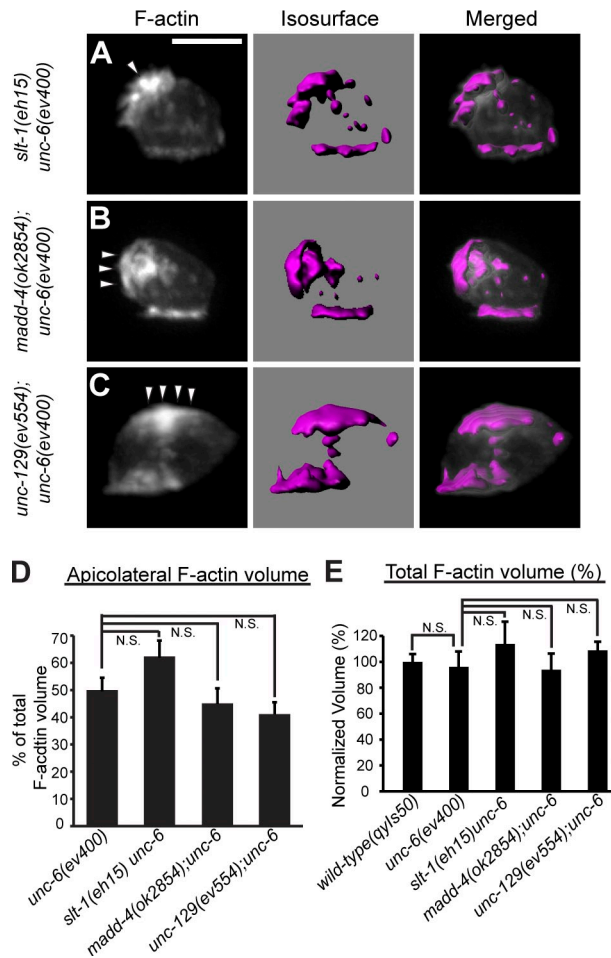


Figure S3. **SLT-1, MADD-4, and UNC-129 do not activate UNC-40.** Anterior is left; ventral is down. (A–C) Images show 3D reconstructions generated from confocal z stacks. Fluorescence (left), corresponding dense F-actin network rendered with isosurfaces (middle), and an overlay (right) are shown. Similar to *unc-6* single mutants, F-actin formed and was mislocalized (arrowheads) to the apical and lateral membranes of the AC in *slt-1 unc-6*, *madd-4; unc-6*, and *unc-129; unc-6* double mutants. Bar, 5  $\mu$ m. (D) The percentage of the volume of F-actin that localized apicolaterally at the P6.p four-cell stage ( $n \geq 12$  per genotype). (E) Quantification of the total F-actin volume in the AC in wild-type animals (control for normalization) and in each of the mutant backgrounds at the P6.p four-cell stage ( $n \geq 12$  per genotype).

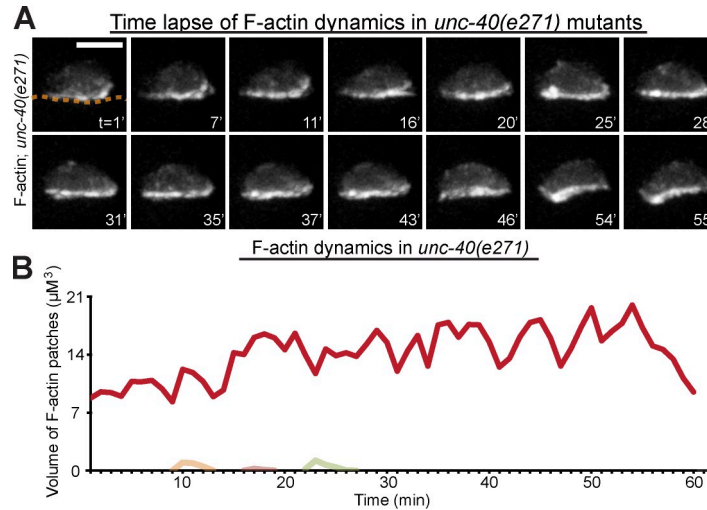


Figure S4. **F-actin is stably polarized in *unc-40* mutants.** Anterior is left; ventral is down. (A) Time-lapse series shows F-actin dynamics in an *unc-40* mutant AC. Time points are indicated in minutes. The broken line denotes the position of the basement membrane in the first frame. Bar, 5  $\mu\text{m}$ . (B) The volume of individual F-actin patches over time within the AC. Each colored line represents a distinct F-actin patch. The red line represents the dominant patch in the basal membrane of the AC. Similar results were observed in  $n = 10/10$  *unc-40* mutants.

Table S1. **Primer sequences and templates used for PCR fusions and cloning**

Primer sequence (5' → 3')	Primer type	Amplicon	Template
TAATGTGAGTTAGCTCACTCATTAGG	Forward	<i>cdh-3</i> promoter	pPD107.94/mk62-63
AACGATGGATACGCTAACAACTTGG	Forward nested	<i>cdh-3</i> promoter	pPD107.94/mk62-63
TTTCTGAGCTCGGTACCTCCAAG	Reverse	<i>cdh-3</i> promoter	pPD107.94/mk62-63
ATGAGTAAAGGAGAAGAAGAACTTTTCAC	Forward	GFP	pPD95.81 (GFP)
GGAAACAGTTATGTTTGGTATATTGGG	Reverse nested	GFP	pPD95.81 (GFP)
AAGGGCCCCGTACGGCCGACTA	Reverse	GFP	pPD95.81 (GFP)
TTGTATAGTTCATCCATGCCATGTG	Reverse for GFP extension to N terminus of protein of interest	GFP	Plasmid <i>cdh-3 &gt; GFP</i>
/5Phos/TTAGCGGCTCCACCAAGTTC	Forward	<i>unc-40</i> ( $\Delta$ FN4/5) for <i>unc-40</i> ( $\Delta$ FN4/5)::GFP	Plasmid <i>unc-40::GFP</i>
/5Phos/AAGTGTTCTGTTCTTTATCTTGCC	Reverse	<i>unc-40</i> ( $\Delta$ FN4/5) for <i>unc-40</i> ( $\Delta$ FN4/5)::GFP	Plasmid <i>unc-40::GFP</i>
TACGGCCGACTAGTAGGAAA	Reverse for fusion	<i>unc-40</i> ( $\Delta$ FN4/5) for <i>unc-40</i> ( $\Delta$ FN4/5)::GFP	Plasmid <i>unc-40::GFP</i>
AATACGTAATGATCACATCAGTATTGCG	Forward	<i>unc-6::nlg-1</i> TM	Plasmid <i>unc-6 &gt; unc-6::nlg-1</i> TM::mCherry
AAGGTACCCCGTTCTTGTGCGATGCGGATA	Reverse	<i>unc-6::nlg-1</i> TM	Plasmid <i>unc-6 &gt; unc-6::nlg-1</i> TM::mCherry
AAGCTTATGATTTGCGACATTTCCGG	Forward	<i>unc-40</i> cDNA for <i>unc-40::mCherry</i>	N2 cDNA
AACCCGGGCTTATCCATACTCGTCTCAA	Reverse	<i>unc-40</i> cDNA for <i>unc-40::mCherry</i>	N2 cDNA

Table S2. **Extrachromosomal array and integrated strain generation**

Strain designation	PCR fusion or plasmids	Injection concentration	Coinjection marker
qyEx257	<i>zmp-5 &gt; unc-6::nlg-1</i> TM::GFP <sup>a</sup>	ng/ $\mu\text{l}$	<i>unc-119+</i> , <i>myo-2 &gt; GFP</i>
qyls155	<i>cdh-3 &gt; unc-40</i> ( $\Delta$ FN4/5)::GFP <sup>b</sup>	10	<i>unc-119+</i> , <i>myo-2 &gt; GFP</i>
qyls262	<i>cdh-3 &gt; unc-40::mCherry</i> <sup>b</sup>	10	<i>unc-119+</i>

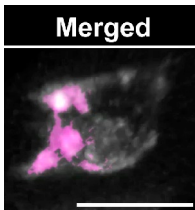
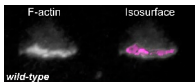
<sup>a</sup>Plasmid.

<sup>b</sup>PCR fusion product.

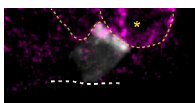
Table S3. Primers used in the screen for *unc-40(qy2)* deletion mutant

Primer sequence (5' → 3')	Primer type	<i>unc-40</i> genomic location of the amplicon
AGTGAGCAGTGCCGAAGAAG	Forward (outer primer)	Region I (4,129–5,345 bp)
CGACAAGTGATAGCCCAGT	Reverse (outer primer)	Region I (4,129–5,345 bp)
CGTACACCTATACGTCCTT	Reverse (poison primer)	Region I (4,129–5,345 bp)
GTAGAAGGTGCTGGGAAGAG	Forward (poison primer)	Region I (4,129–5,345 bp)
GCGCTGTACATGTGACTACA	Forward (inner primer)	Region I (4,129–5,345 bp)
CGATAGAAGCACGTGAGACA	Reverse (inner primer)	Region I (4,129–5,345 bp)
TGTCTCACGTGCTTCTATCG	Forward (outer primer)	Region II (5,301–6,694 bp)
AGGTTGTCCTCCACTTGGTG	Reverse (outer primer)	Region II (5,301–6,694 bp)
GCAGCCACTGATGATGAATC	Reverse (poison primer)	Region II (5,301–6,694 bp)
CCTCAGGAGTTCCAATGACT	Forward (poison primer)	Region II (5,301–6,694 bp)
ACTGGGCTATACACTTGTGCG	Forward (inner primer)	Region II (5,301–6,694 bp)
GCTCCAACGGATGTCAATCG	Reverse (inner primer)	Region II (5,301–6,694 bp)
CGATTGACATCCGTTGGAGC	Forward (outer primer)	Region III (6,654–8,226 bp)
GTAGTCCTTCCACAGTAGCC	Reverse (outer primer)	Region III (6,654–8,226 bp)
GCTGGTGGAAAGCCATGATAC	Reverse (poison primer)	Region III (6,654–8,226 bp)
GGATGGGGATTGAGTGTCC	Forward (poison primer)	Region III (6,654–8,226 bp)
CACCAAGTGAGGACAACCT	Forward (inner primer)	Region III (6,654–8,226 bp)
GTCTCGGTGCTATTCACGTA	Reverse (inner primer)	Region III (6,654–8,226 bp)
TACGTGAATAGCACCGAGAC	Forward (outer primer)	Region IV (8,184–9,554 bp)
GTGACTACAGCCTTGGCTCT	Reverse (outer primer)	Region IV (8,184–9,554 bp)
CCTATTCCACCTCCACTTCC	Reverse (poison primer)	Region IV (8,184–9,554 bp)
GGTCTTGGAGGTCCACCTAA	Forward (poison primer)	Region IV (8,184–9,554 bp)
GGCTACTGTGGAAGGACTAC	Forward (inner primer)	Region IV (8,184–9,554 bp)
ACTAATGCTCAACCGGCTC	Reverse (inner primer)	Region IV (8,184–9,554 bp)

Video 1. **F-actin dynamics in wild-type, *unc-40*, and *unc-6* mutant ACs.** The time lapse shows F-actin (visualized with *cdh-3 > mCherry::moeABD* in grayscale [left] and isosurface renderings in magenta [right]) in the *C. elegans* AC. In wild-type and *unc-40* mutants, F-actin is dynamic, but localized tightly to the basal cell membrane. In contrast, in *unc-6* mutants, F-actin localizes in dynamic clusters that form and then break down in all membrane domains of the cell. Images in movies were created from 3D reconstructions generated from confocal z stacks (CSU-10 spinning disc confocal microscope; Yokogawa Electric Corporation). Frames were acquired at 1-min intervals for a total of 60 min. The movies correspond to animals shown in Fig. S4 (A and B) and Fig. 4 D, respectively. Bar, 5  $\mu$ m. Anterior is left and ventral is down.

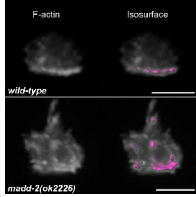
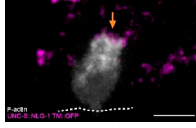


Video 2. **F-actin colocalizes with UNC-40 in *unc-6* mutants.** The time lapse shows that UNC-40::GFP (left) and F-actin (*cdh-3 > mCherry::moeABD*; middle) have persistent colocalization (highlighted in magenta, right; colocalization merged with UNC-40::GFP, far right) in the *C. elegans* AC's apical and lateral membranes in *unc-6(ev400)* mutants. Frames were acquired at 1-min intervals for a total of 75 min using a spinning disc confocal microscope (CSU-10; Yokogawa Electric Corporation). Imaris colocalization function (Coloc) was used to set a threshold for each fluorophore in reconstructed 3D images. The voxels containing both GFP and mCherry signal were considered colocalized. Bar, 5  $\mu$ m.



Video 3. **Dorsally localized UNC-6 orients and stabilizes UNC-40 in *unc-6* mutants.** The time lapse shows that ectopic membrane-tethered UNC-6 (*zmp-5 > unc-6::nlg-1 TM::GFP*; magenta) expressed in the dorsal *C. elegans* uterine cells (yellow broken lines; the asterisk indicates the cell with high constant expression of UNC-6) stably orients F-actin (grayscale; white arrow) to the AC's apical cell membrane in contact with UNC-6 in *unc-6(ev400)*. Frames were acquired at 1-min intervals for a total of 58 min using a spinning disc confocal microscope (CSU-10; Yokogawa Electric Corporation). The basement membrane is indicated with a white broken line. Bar, 5  $\mu$ m.

Video 4. **UNC-40 reorients F-actin toward a changing source of UNC-6.** The time lapse shows an AC initially directing polarity (visualized with the F-actin probe *cdh-3 > mCherry::moeABD*; grayscale) toward a dorsal *C. elegans* uterine cell expressing membrane-tethered UNC-6 (magenta; orange arrow). When the AC made contact with a new source of localized UNC-6 on a neighboring anterior dorsal uterine cell, a polarized response (yellow arrow) was directed toward this new source of UNC-6. Further, as UNC-6 protein was lost on the posterior dorsal uterine cell, polarity was lost here (orange arrowhead). The basement membrane is indicated with a white broken line. Frames were acquired at 1-min intervals for a total of 72 min using a spinning disc confocal microscope (CSU-10; Yokogawa Electric Corporation). The movie covers the time series shown in Fig. 6 (D and E). Bar, 5  $\mu$ m.



Video 5. **MADD-2 promotes UNC-40-mediated F-actin polarization toward UNC-6.** The time lapse shows F-actin (visualized with *cdh-3 > mCherry::moeABD* in grayscale [left] and overlaid with isosurface renderings in magenta [right]) in the *C. elegans* AC. In a representative wild-type animal, F-actin was dynamic but consistently polarized to the basal AC membrane. In contrast, in a *madd-2* animal, transient F-actin patches were mislocalized to the apical and lateral AC membrane. Frames were acquired at 1-min intervals for a total of 60 min using a spinning disc confocal microscope (CSU-10; Yokogawa Electric Corporation). The movies cover the time series shown in Fig. 8 (B and E, respectively). Bars, 5  $\mu$ m.